Hierarchical Assembly of a Series of Rod−Coil Block Copolymers: Supramolecular LC Phase in Nanoenviroment

Christopher Y. Li,*,† Kishore K. Tenneti,† Dong Zhang,‡ Hailiang Zhang,‡ Xinhua Wan,*,‡ Er-Qiang Chen,‡ Qi-Feng Zhou,*,‡ Avila-Orta Carlos,§ Sics Igos,§ and Benjamin S. Hsiao§

Department of Materials Science and Engineering, Drexel University, Philadelphia, Pennsylvania 19104; Department of Polymer Science, Peking University, P. R. China; and Department of Chemistry, State University of New York at Stony Brook, Stony Brook, New York 11794

Received October 2, 2003; Revised Manuscript Received January 13, 2004

ABSTRACT: A series of narrowly distributed rod−coil diblock copolymers, poly(styrene-*block*-(2,5-bis-[4-methoxyphenyl]oxycarbonyl)styrene) (PS−PMPCS), were synthesized by 2,2,6,6-tetramethyl-1-piperidinyloxy (TEMPO)-mediated living free radical polymerization. Differential scanning calorimetry, wide-angle X-ray diffraction, small-angle X-ray scattering, polorized light microscopy, and transmission electron microscopy were used to study the phase structure of this series of rod−coil polymers. It was found that the block copolymers microphase separate into ordered structures at temperatures below ca. 240 °C. PMPCS blocks form supramolecular columnar nematic phase (ϕ_N) within the microphase-separated block copolymers. LC columnar axes were identified to be parallel to the block copolymer lamellar normal. Two layers of LC columns are confined in each LC domain, and the hierarchical structure resembles the "bilayer smectic A" phase observed in small molecular liquid crystals and rod−coil oligomers.

Introduction

Liquid crystalline (LC) block copolymers play a major role in creating hierarchical self-assembled structures in different length scales.[1] In these systems, microphase separations occur on the scale of 10−100 nm range. LC molecules form "sublevel" LC structures within these ordered nanodomains. The structural dimension of the LC ordering is around 1−5 nm, which is 1 order of magnitude lower than the dimension of block copolymer phase structures. Hierarchical structures can thus be formed. A number of research groups have systematically studied the self-assembly behavior of LC block copolymers, and hierarchical structures involving one-dimensional (1-D) smectic LC phases confined in different block copolymer structures have been successfully achieved.[1]

Most of the LC block copolymer studies focus on "terminally linked" side-chain LC polymers, in which one end of the LC mesogens is attached to the polymer backbones through "soft" spacers, such as methylene groups.[2−7] By laterally linking the "waist" of LC mesogens directly to polymer backbones (without spacers), mesogenic jacketed LC polymers (MJLCP) can be achieved.[8] Because of the semirigid nature of the polymer chains induced by the strong interaction between the side-chain mesogens and the polymer backbone, MJLCPs could serve as "rods" to form rod−coil block copolymers, which represent a new category of self-assembling copolymers that combine microphase separation of coil−coil block copolymers and orientational ordering of rod segments.[9] Compared to the thoroughly investigated coil−coil block copolymer systems, many issues in rod−coil block copolymer systems still remain unsolved. A few rod−coil macromolecules, including diblock copolymers with polypeptides,[10] poly(*p*-phenylene),[11] poly(phenylquinoline),[12] and poly(hexyl isocyanate)[9a,13] as rod blocks, have been reported. The microphase separation characteristic of poly(styrene)-*block*-poly(hexyl isocyanate) (PS−PHIC) has been systematically investigated, and a number of novel morphologies such as "wavy lamellar", "zigzag", and "arrowhead" have been observed.[1a,9a,13] Exotic self-assembly behavior has also been observed in a number of rod−coil oligomer systems with LC oligomers as the rod segments.[9b,c,14]

Recently, using MJLCP as the rod block, a new series of rod−coil block copolymers, poly(styrene-*block*-(2,5-bis-[4-methoxyphenyl]oxycarbonyl)styrene) (PS−PMPCS), have been synthesized, and their solution self-assembly behavior has been investigated.[15] Morphology and rheological behavior of rod−coil poly(styrene)-*block*-poly(2,5-bis(4-butylbenzoyl)oxystyrene) (PS−PBBOS) has also been reported.[16] In this Article, we report, for the first time, the hierarchically ordered rod−coil diblock copolymer structures with MJLCPs as the rod blocks. The confined LC phase behavior within the microphase-separated block copolymers will be discussed.

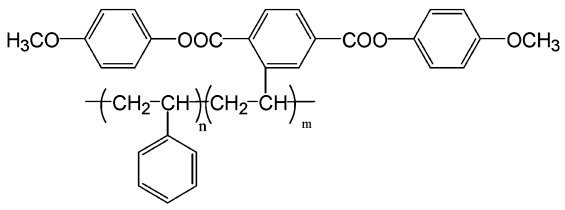

PS-PMPCS

Experimental Section

Materials and Sample Preparation. The design and synthesis of the PS−PMPCS block copolymers were reported previously.[8a−c] The number-average molecular

† Drexel University.
‡ Peking University.
§ SUNY Stony Brook.
* To whom correspondence should be addressed. E-mail: chrisli@drexel.edu; xhwan@pku.edu.cn; qfzhou@pku.edu.cn.

10.1021/ma0354905 CCC: $27.50
Published on Web 03/17/2004

Table 1. Molecular Analysis of PS−PMPCS Rod−Coil Block Copolymers

sample ID	sample	M_n(St)[a]	M_n(PMPCS)[b]	M_n (total)	M_w/M_n	f_{PMPCS}
PS−PMPCS1	$PS_{109}-PMPCS_{27}$	11 378	10 935	22 313	1.13	0.44
PS−PMPCS2	$PS_{109}-PMPCS_{41}$	11 378	16 573	27 951	1.18	0.54
PS−PMPCS3	$PS_{171}-PMPCS_{34}$	17 800	13 625	31 425	1.18	0.38
PS−PMPCS4	$PS_{227}-PMPCS_{47}$	23 600	18 800	42 400	1.24	0.39
PMPCS	$PMPCS_{50}$		20 100	20 100	1.20	1

[a] PS molecular weights were measured by SEC calibrated with PS standards. [b] PMPCS molecular weight was estimated using NMR method (see Experimental Section).

Scheme 1. Schematic Representation of the Shear Geometry for the PS−PMPCS Block Copolymers

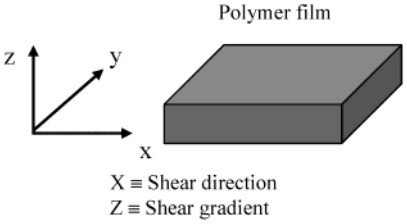

weight (M_n) and the polydispersity (M_w/M_n) were estimated from size exclusion chromatography (SEC, Waters 150C) profiles and calibrated with standard PS. The copolymer composition was determined by nuclear magnetic resonance (NMR) spectroscopy (^{1}H NMR, 400 MHz) with dichloromethane-d_2 as solvent. The block length was estimated from the intensity ratio of the methoxy groups ($\delta = 3.3-3.8$) and the aromatic groups ($\delta = 6.3-7.2$). Sample information such as molecular weights, polydispersity, and volume fraction can be found in Table 1.

Sheared samples were obtained by solution-casting thick polymer films (thickness ~ 0.5−1 mm) from 5% (w/w) chloroform solutions. The solvent was allowed to evaporate at room temperature for 2 days. Residual solvent was removed under vacuum at 80 °C, and the sample was then annealed at 145 °C for 24 h to allow microphase separation. To achieve uniform shear alignment of the microdomains, the microphase-separated samples were then subject to a large-amplitude reciprocating shear at 140 °C for ~20 min. The shear frequency was ~0.5 Hz, and the shear amplitude was ~150%. The shear direction was along the *x* axis as shown in Scheme 1, and the shear gradient was along the *z* axis. The resulting polymer film was then taken out of the shearing apparatus and quenched to room temperature. The samples were then annealed at 140 °C for an additional 8 h to release any possible residue shear stress. The final film thickness was ~0.2−0.3 mm.

Equipment and Experiments. Differential scanning calorimetry (DSC), small-angle X-ray scattering (SAXS), wide-angle X-ray diffraction (WAXD), transmission electron microscopy (TEM), and polarized light microscopy (PLM) were employed to characterize structure and morphology of the block copolymer. The thermal transitions were detected using a Perkin-Elmer DSC-7. The temperature and heat flow were calibrated using standard materials at different cooling and heating rates between 5 and 40 °C/min. Samples with a typical mass of 3 mg were encapsulated in sealed aluminum pans. A controlled cooling experiment was always carried out first, and a subsequent heating was performed at a rate that was equal to or faster than the previous cooling.

Two-dimensional (2-D) SAXS experiments were carried out on the synchrotron X-ray beamline X-27C at the National Synchrotron Light Source in Brookhaven National Laboratory. The wavelength of the X-ray beam was 0.1307 nm. The zero pixel of the 2-D SAXS pattern was calibrated using silver behenate, with the first-order scattering vector q ($q = 4\pi \sin\theta/\lambda$, where λ is the wavelength and 2θ the scattering angle) being 1.076 nm^{-1}. The air scattering was subtracted. The X-ray beam spot dimension was 0.1 mm in diameter. The X-ray beam was aligned parallel to the *x*, *y*, and *z* directions of the sample (see Scheme 1).

2-D WAXD patterns were recorded at room temperature for different exposure times using an imaging plate equipped with an 18 kW X-ray rotating anode generator (Cu Kα radiation, Rigaku automated X-ray imaging system with 1500 × 1500 pixel resolution). The air scattering was subtracted from the WAXD patterns.

TEM experiments were carried out using a JEOL 2000FX TEM with an accelerating voltage of 200 kV. A Reichert Ultracut cryo-ultramicrotome was used to microtome the sheared block copolymer sample. Thin sections of ~50 nm were microtomed at room temperature and collected on TEM grids, followed by staining in RuO_4 vapor for approximately 30 min. PS microdomains were preferentially stained, and the mass contrast was therefore enhanced.

LC texture was examined via a PLM (Olympus BX-51) coupled with Mettler hot stage (FP 82 HT with a FP-90 central processor). The image was captured using an Insight digital camera. The film thickness was controlled to be ~10 μm, prepared by both solution-casting and melt-pressing methods. The specimens were slightly sheared (shear rate ~1 Hz, shear amplitude ~20−50%) to increase LC domain sizes.

Results and Discussion

Figure 1a shows DSC cooling thermograms (cooling rate 20 °C/min) of PMPCS and four PS−PMPCS samples (as listed in Table 1). One broader transition can be identified in the temperature region ~135−100 °C for PMPCS homopolymer and ~135−90 °C for all of the block copolymer samples. Subsequent heating thermograms at 20 °C/min show that this broad transition might be due to two overlapped glass transitions located at around 100−102 and 116−117 °C, although these two glass transitions are not clear. We therefore recorded fast heating thermograms (40 °C/min heating) of slow cooled samples (2.5 °C/min cooling), as shown in Figure 1b. It is known that fast heating of slow cooled samples could induce endothermic hysteresis peaks at the glass transition region, which, in turn, make the glass transition more evident.[17] As indicated by the arrows in Figure 1b, the two endothermic hysteresis peaks of PS and PMPCS glass transitions can be clearly observed. The glass transition temperatures of PMPCS and PS−PMPCS are listed in Table 2. It should be noted that in these block copolymers both the PS and PMPCS blocks possess higher glass transition temperatures than those

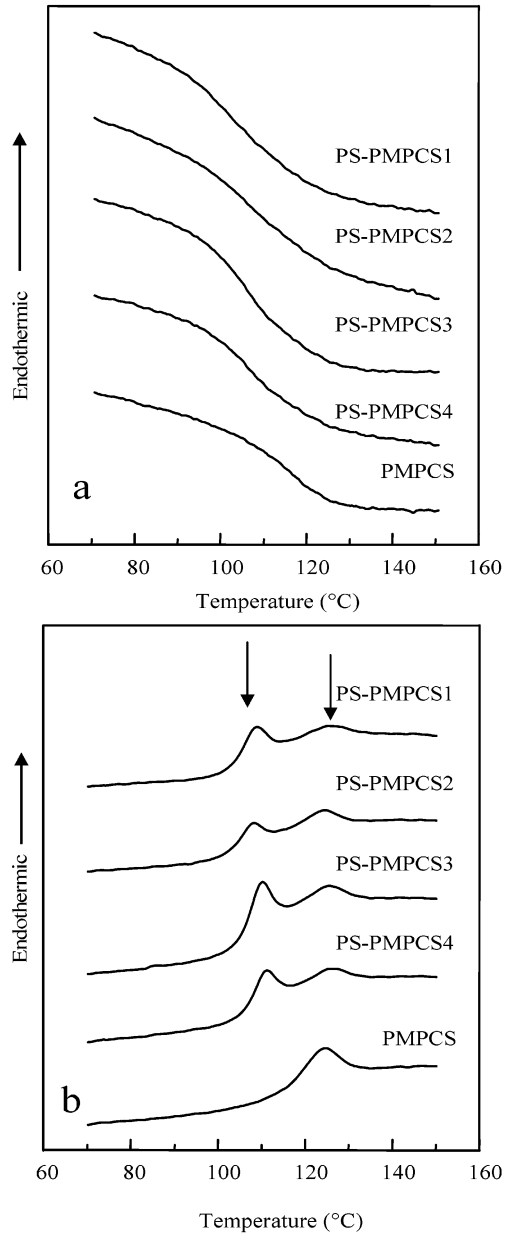

Figure 1. DSC thermograms of PMPCS and PS−PMPCS 1−4 (a) cooling at 20 °C/min and (b) heating at 40 °C/min (samples were cooled at 2 °C/min from 220 °C). Two hysteresis peaks of PS and PMPCS blocks can be clearly observed for PS−PMPCS block copolymers, indicating two glass transitions of phase-separated PS and PMPCS blocks, respectively.

Table 2. Glass Transition Temperatures and Lamellar *d* Spacings of PS−PMPCS Block Copolymers

sample ID	sample	T_g^{PS} (°C)	T_g^{PMPCS} (°C)	*d*-spacing (nm)[a]
PS−PMPCS1	PS_{109}−$PMPCS_{27}$	100.1	117.5	17.5
PS−PMPCS2	PS_{109}−$PMPCS_{41}$	100.0	116.5	24.9
PS−PMPCS3	PS_{171}−$PMPCS_{34}$	102.4	117.0	26.9
PS−PMPCS4	PS_{227}−$PMPCS_{47}$	102.5	116.4	34.7
PMPCS	$PMPCS_{50}$		113.2	

[a] Determined by SAXS experiments.

in their corresponding homopolymers. This might be due to the confinement effects: both the PS and PMPCS are confined by each other in the microphase-separated sample films. The detailed mechanism of the confinement effects on glass transitions is currently under investigation. No distinct first-order transition peaks have been identified from the DSC nonisothermal experiments running from room temperature to 220 °C.

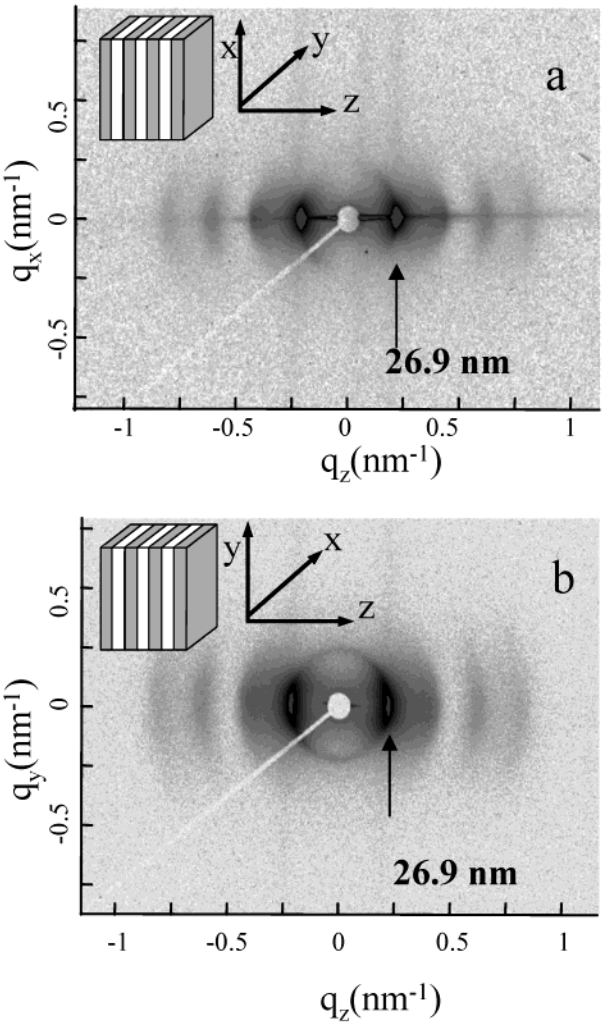

Figure 2. 2-D SAXS patterns of a PS_{171}−$PMPCS_{34}$ film with X-ray along (a) the *y* direction and (b) the *x* direction. The insets show the schematic representations of the lamellar phase with the correct orientation. *X* is the shear direction as defined in Scheme 1.

A set of 2-D SAXS patterns of a mechanically sheared PS_{171}−$PMPCS_{34}$ film were recorded as shown in Figure 2. The X-ray beam was along either the *y* (Figure 2a) or the *x* (Figure 2b) direction of the sample. In both cases, the horizontal axes (equator) were along the *z* direction of the film. It is evident that up to the fourth order of the diffraction can be seen, and the *d* spacings obey the ratio of 1:2:3:4. A lamellar structure of the microphase-separated PS_{171}−$PMPCS_{34}$ can thus be identified, and the *d* spacing of the lamella was calculated to be 26.9 nm. For the four PS−PMPCS samples that have been investigated, the SAXS patterns share similar features, and lamellar structures can always be observed. The *d* spacings of the lamellar order are listed in Table 2. The volume fractions of PMPCS blocks in these four block copolymers are between 0.38 and 0.54, which falls into the conventional volume fraction range for a lamellar structure in coil−coil diblock copolymers. Since the observed diffractions were along the q_z direction in both parts a and b of Figure 2, it can be concluded that the lamellar normal is parallel to the mechanical shear gradient (the *z* direction), which is consistent with the previous reports on the coil−coil block copolymers.[18]

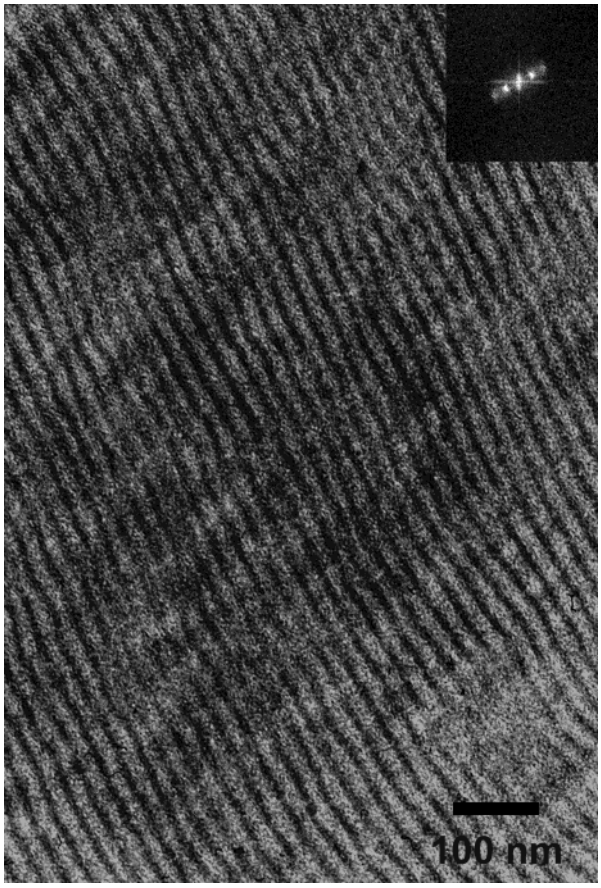

Figure 3. TEM micrograph of a thin section of PS_{109}−$PMPCS_{41}$. The sample was sectioned along the *yz* plane followed by RuO_4 staining for 30 min. The dark regions are PS domains, which were stained by RuO_4.

The real space schematic representations of the lamellar structures are shown in the insets of Figure 2a,b.

The lamellar nature of the block copolymer can also be supported by TEM experiments. A thin section of PS_{109}−$PMPCS_{41}$ was obtained by microtoming sheared polymer films along the *yz* plane. The thin section was collected on a TEM grid and subjected to RuO_4 vapor staining for 30 min. Figure 3 shows a TEM micrograph of such a thin section. Relatively uniform lamellar structure can be seen and the inset is a Fourier transform of this image, which indicates that long-range order of the lamellar structure has been achieved by mechanical shearing. The *d* spacing of the lamellae can be measured to be ∼24.3 nm, which is consistent with the SAXS observation of 24.9 nm for PS_{109}−$PMPCS_{41}$ (see Table 2).

2-D WAXD was employed to determine the LC phase structure of the shear oriented PS−PMPCS films. Three 2-D WAXD patterns of PS_{171}−$PMPCS_{34}$ were obtained with different zone directions: i.e., the X-ray beam was along the *y*, *x*, and *z* directions, as shown in parts a, b, and c of Figure 4, respectively. Two distinct diffractions can be observed in all these three patterns: the low-angle diffraction arcs/circle and the diffused scattering in the wide-angle region. In Figure 4a,b, the X-ray patterns show orientated LC structures. The low-angle diffractions are located on the meridian while the wide-angle amorphous scattering are located on the equator. Figure 5 shows an azimuthal scan of Figure 4a, indicating that relatively good orientation of the LC phase has been obtained. Figure 4c, on the other hand, shows random orientation in both the low-angle and the wide-angle regions. Detailed analysis of the LC orientation will be discussed in the following section. It is noteworthy that in all these three X-ray patterns relatively weak random PS amorphous scattering can be observed between the low-angle diffraction arcs and the wide-angle amorphous scattering, as indicated by the arrows in Figure 4.[19]

The LC nature of the MJLCPs has been investigated in a number of systems, and most of the X-ray experiments demonstrated similar diffraction patterns as those shown in Figure 4. Because of the absence of the high-order diffraction at the low-angle region, both smectic and nematic phases were proposed.[8] In a nematic LC phase, low-angle X-ray diffraction can always be observed, and the *d* spacing of the diffraction corresponds to the molecular length.[20] In the present case, an extended MPCS mesogen has a length of ∼1.9 nm, and the low-angle diffraction has a *d* spacing of 1.5 nm (the same *d* spacing as the X-ray pattern of the PMPCS homopolymer). The differences between the calculated mesogen length and the diffraction *d* spacing indicate that the observed low-angle diffractions do not represent the molecular length of the PMPCS side chain. It is therefore less likely that PMPCS has a normal molecular nematic phase. To explain the relatively "short" *d* spacing (compared to the mesogen length) in the low-angle region, one might propose a possible nematic phase with smectic C fluctuation,[21] which involves the mesogen tilting with respect to the fluctuation layers. Tilting of the mesogen groups could induce a shorter layer *d* spacing. However, in Figure 4a,b, the lower angle reflections are located on the meridian, and the amorphous scattering is located on the equator. In the case of a nematic phase with smectic C fluctuation, quadrant diffractions are expected. To explain the WAXD pattern, a supramolecular columnar nematic phase (Φ_N) is proposed for the PMPCS blocks. Since the bulky side mesogens are directly linked to the main chain of the polymer, which causes the main chain to be (close to) extended, the entire PMPCS block forms a column with a diameter of 1.5 nm, corresponding to the low-angle diffraction arcs in Figure 4. Assuming that the 1.5 nm *d* spacing is due to the tilting of the mesogen, the tilting angle can be calculated to be ∼38° (based on extended conformation of MPCS). Therefore, it is the macromolecular columns, instead of the mesogen groups, that possess the nematic orientational order, and the LC phase can be defined as the supramolecular Φ_N phase. The column formation of PMPCS also ensures the "rod" nature of LC blocks, and thus, these PS−PMPCS samples can be considered as rod−coil diblock copolymers. It should be noted that columnar hexagonal phase has been reported recently in the case of poly[di-(4-heptyl) vinylterephthalate] and poly[di(alkyl) vinylterephthalates], where similar supramolecular columns are formed. Those columns, however, are packed with higher hexagonal order, and the X-ray patterns show distinct second- and third-order peaks with a ratio of $1:\sqrt{3}:2$.[22]

Since the low-angle diffractions are due to the intercolumnar diffraction (the orientation of the diffraction should be perpendicular to the columnar axis), one can therefore deduce the columnar orientation within the sheared film by analyzing three diffraction patterns in Figure 4: in Figure 4a,b, the X-ray was perpendicular to the columnar axes. The well-oriented low-angle arcs

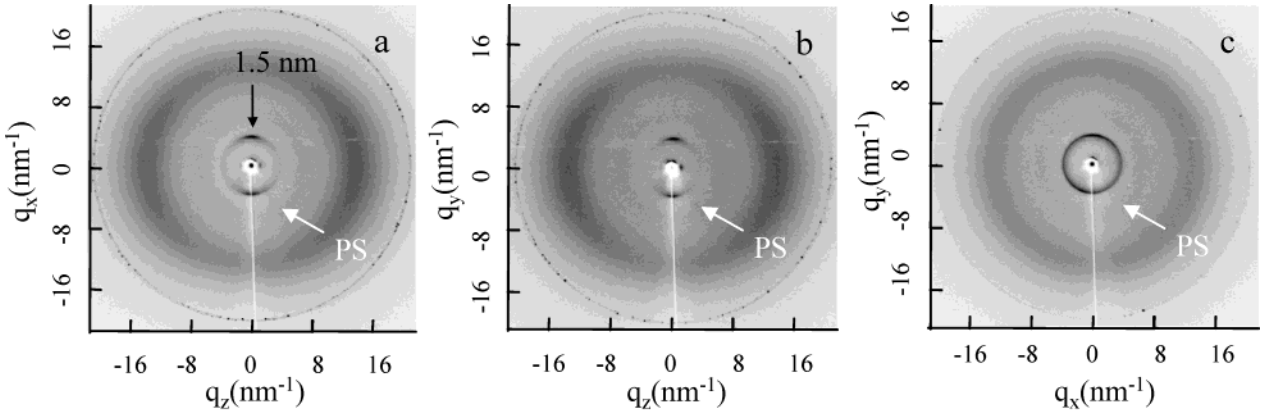

Figure 4. 2-D WAXD of a PS_{171}−$PMPCS_{34}$ film with X-ray beam along (a) the *y*, (b) the *x*, and (c) the *z* direction. *X* is the shear direction as defined in Scheme 1.

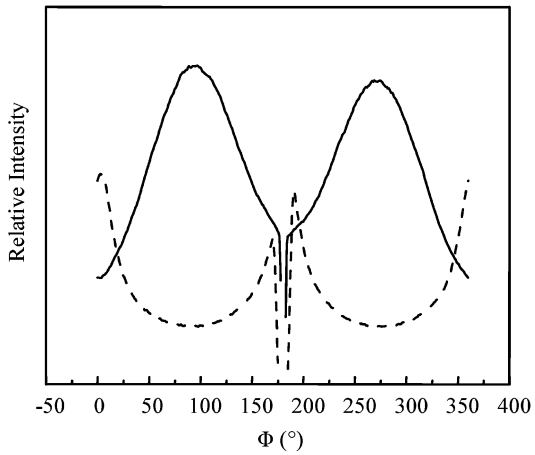

Figure 5. Azimuthal scan profile of the low-angle (dotted line) and wide-angle (solid line) reflections in Figure 4a.

can be observed, and since the arcs are located on the meridian, the columns should be parallel to the *z* direction, which corresponds to the equator in the 2-D WAXD pattern. In the case of Figure 4c, the X-ray was parallel to the columnar axes, and an isotropic ring of the low-angle diffraction can be observed. The columns are thus perpendicular to the *xy* plane, and they are parallel to the *z* axis. According to the Scherrer equation,[23] the correlation length perpendicular to the column direction can be calculated to be ∼20 nm, corresponding to ∼13−14 columns. In relatively higher ordered columnar hexagonal phase of similar MJLCPs, a correlation length as high as 120 nm has been reported.[22]

LC phase formation in this series of block copolymers can also be confirmed by PLM experiments. The schlieren texture was observed for all the block copolymer samples, and Figure 6 shows one example observed for PS_{109}−$PMPCS_{27}$ at 150 °C. The block copolymer was hot pressed at 200 °C and slightly sheared to increase the monodomain size. The shear direction is parallel to one of the polarizers, and the schlieren texture is stable up to 240 °C.

Combining both the WAXD and SAXS results, the hierarchical packing scheme of the PS−PMPCS rod−coil diblock copolymers can be schematically illustrated in Figure 7. PMPCS blocks form the rods with a diameter of 1.5 nm while PS blocks form the coil (Figure 7b). These rod−coil blocks pack together forming a layer structure (Figure 7c), and the rod axes are parallel to

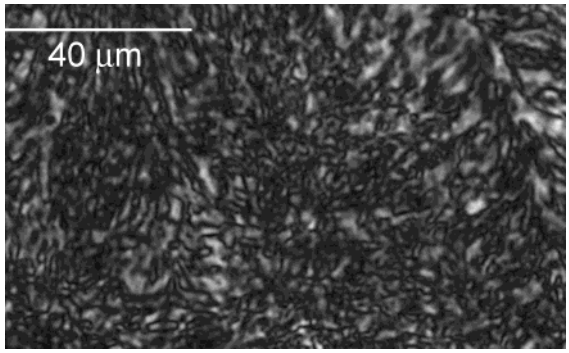

Figure 6. LC schlieren texture of PS_{109}−$PMPCS_{27}$ taken at 150 °C.

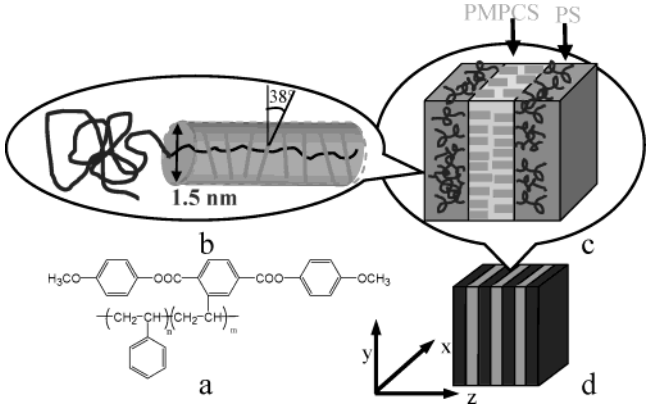

Figure 7. Schematic representations of PS−PMPCS hierarchical structure. (a) Chemical structure of PM-PMPCS. (b) The PMPCS blocks form columns, while PS blocks form the flexible coils. (c) PMPCS rods and PS coils microphase separate into lamellar phase, and the rods are parallel to the layer normal. There are two layers of rods in each PMPCS layer. (d) PS−PMPCS lamellar structure.

the lamellar normal. According to the molecular weight of PMPCS and the lamellar *d* spacing, assuming zigzag conformation of the PMPCS backbones (which is close to the real case due to the bulky mesogen groups), it can be concluded that within each PMPCS domain two layers of the macromolecular columns can be formed, indicating a bilayer structure. The bilayer structure can be further supported by comparing the *d* spacings of PS_{109}−$PMPCS_{41}$ and PS_{109}−$PMPCS_{27}$, both of which have the same PS block lengths. The difference of the lamellar spacings (24.9 nm vs 17.5 nm) corresponds to twice of the molecular length difference of $PMPCS_{27}$ and $PMPCS_{41}$ in extended conformations. Figure 7d shows

the block copolymer lamellar structure. It is noteworthy that in the present rod−coil system, due to the microphase separation of PS and PMPCS, PMPCS segments are confined within PS lamellae and are forced to form layer structures (Figure 7c), which certainly do not exist in the unconfined Φ_N phase.

Of interest is, due to the "rod" nature and liquid crystallinity of the PMPCS blocks, to compare the present samples with other rod−coil molecular systems. The most thoroughly investigated rod−coil polymer system is PS−PHIC.[1a,9a,13] A number of interesting morphologies such as wavy lamellar, zigzag, and arrowhead have been observed. In the PS−PHIC system, depending upon the volume fractions of the "rods", the PHIC rods are known to be bilayer/interdigitated and tilted. The smectic C phase with layer spacing higher than 190 nm has been associated with the zigzag morphology, and the arrowhead morphology resembles the small LC smectic O phase. Accordingly, if we consider the PMPCS rods as the "mesogens" and PS blocks as the "soft tails", a bilayer smectic A phase can be assigned to the present series of PS−PMPCS samples. The bilayer smectic A packing has been found in a number of small molecular liquid crystals and rod−coil oligomers.[9c] The "rods" (molecular columns) are perpendicular to the lamellar layer as shown in Figure 7, and they are not interdigitated. The interdigitation in PS−PHIC systems is due to the packing requirement at the interface of PS and PHIC. The area per junction for the PHIC rod was estimated to be ~1 nm^2 and is independent of the molecular weight. Assuming strong segregated lamellar diblocks, e.g., in the case of PS-polydiene, the area per chain of PS varies as $0.14M^{1/3}$ nm^2 (M: molecular weight, g/mol).[9a] For PS with M_n higher than 10 000 g/mol (the case of PS_{104}−$PHIC_{73}$ in ref 9a), the area per chain of PS is ~3.01 nm^2, much larger than that of the PHIC; interdigitation can partially solve the packing problem caused by the junction area mismatch. In the case of PS−PMPCS, however, assuming a columnar diameter of 1.5 nm, the molecular column has an approximate 2 nm^2 cross-area per junction, which doubles the value of PHIC. A noninterdigitated bilayer structure may thus be stabilized in the PS−PMPCS system. It should be noted that the bilayer model also can be observed in PS_{14}−$PHIC_{36}$ and PS_7−$PHIC_{58}$; in both cases, the PS blocks have small areas per junction.[9a]

Also of interest is that the azimuthal position of the low-angle diffraction arcs in Figure 4a,b: the diffraction arcs are parallel to the x and y directions, respectively. Since the lamellar layers (the xy plane) are parallel to the shear direction, according to these two patterns, one might conclude that the macromolecular columns are perpendicular to shear direction and the mesogens are more or less parallel to the lamellar layer (38° away from lamellar layers). It is evident that shear has induced the lamellar layer orientation while it does not have any direct effect on the supramolecular LC orientation. It is known that shearing the MJLCP homopolymers generates an X-ray pattern with the low-angle diffraction perpendicular to the shear direction, indicating that shear will directly align macromolecular columns,[8] and the LC orientation depends on parameters such as molecular weight, temperature, and shear rate.[24] In the present case, the difference of shear behaviors of the PMPCS homopolymer and PS−PMPCS block copolymers might be due to the shear rate employed in the sample preparation. Relatively slow shear rate (0.5 Hz) was used for achieving the block copolymer orientation, and high shear rate (10 Hz) was employed to orientate LC homopolymers. Quantitative study is ongoing to illustrate the role of shear rate as well as PS confinement effects in PMPCS LC orientation.

Summary

Phase structures and morphologies of a series of rod−coil block copolymer PS−PMPCS have been investigated using DSC, PLM, SAXS, WAXD, and TEM techniques. It has been found that this series of PS−PMPCS samples possess lamellar microphase structure, and the lamellar d spacing increases with increasing both of the PS and PMPCS molecular weights. The glass transition temperatures of the PMPCS and PS blocks are higher than those in their corresponding homopolymers. The PMPCS rigid columns are formed due to the strong interaction between the side-chain mesogens and the polymer backbones. The macromolecular columns possess orientational order, and columns are parallel to the lamellar normal. The packing of the rod−coil block resembles a "bilayer smectic A" molecular structure observed in small molecular liquid crystals and rod−coil oligomers. The reported results demonstrated a new series of hierarchically ordered rod−coil diblock copolymers. Phase structures of this series of polymers with different rod volume fractions are currently under investigation.

Acknowledgment. This work was supported by the National Science Foundation (NSF CAREER award, DMR-0239415), ACS-PRF, and 3M Corp. C.Y.L. is grateful to Prof. S. Z. D. Cheng for his continuous support and enthusiastic discussions. X.H.W. and Q.F.Z. thank the National Natural Science Foundation of China (No. 20274001 and 20134010) for financial support.

References and Notes

(1) (a) Muthukumar, M.; Ober, C. K.; Thomas, E. L. *Science* **1997**, *277*, 1225. (b) Chiellini, E.; Galli, G.; Angeloni, A. S.; Laus, M. *Trends Polym. Sci.* **1994**, *2*, 244. (c) Adams, J.; Gronski, W. *Polym. Prepr.* **1989**, *30*, 446. (d) Mao, G.; Ober, C. K. *Handb. Liq. Cryst.* **1998**, *3*, 66. (e) Adams, J.; Gronski, W. *Makromol. Chem. Rapid Commun.* **1989**, *10*, 553.

(2) For side chain LC, see: (a) Percec, V.; Pugh, C. Molecular engineering of predominantly hydrocarbon-based LCPs. In McArdle, C. B., Ed.; *Side Chain Liquid Crystalline Polymers*; Blackies: Glasgow, 1989. (b) Arehart, S. V.; Pugh, C. *J. Am. Chem. Soc.* **1997**, *119*, 3027. (c) Pugh, C.; Bae, J. Y.; Dharia, J.; Ge, J. J.; Cheng, S. Z. D. *Macromolecules* **1998**, *31*, 5188. (d) Pugh, C.; Shao, J.; Ge, J. J.; Cheng, S. Z. D. *Macromolecules* **1998**, *31*, 1779.

(3) (a) Fisher, H.; Poser, S.; Arnold, M.; Frank, W. *Macromolecules* **1994**, *27*, 7133. (b) Fisher, H.; Poser, S.; Arnold, M. *Liq. Cryst.* **1994**, *8*, 503. (c) Fisher, H.; Poser, S.; Arnold, M. *Macromolecules* **1995**, *28*, 6957.

(4) (a) Tian, Y. Q.; Watanabe, K.; Kong, X. X.; Abe, J.; Iyoda, T. *Macromolecules* **2002**, *35*, 3739. (b) Omenat, A.; Hikmet, R. A. M.; Lub, J.; van der Sluis, P. *Macromolecules* **1996**, *29*, 6730.

(5) (a) Mao, G.; Wang, J.; Clingman, S. R.; Ober, C. K.; Thomas, E. L.; Chen, J. T. *Macromolecules* **1997**, *30*, 2556. (b) Mao, G.; Wang, J.; Ober, C. K.; Brehmer, M.; O'Rourke, M.; Thomas, E. L. *Chem. Mater.* **1998**, *10*, 1538. (c) Osuji, C. O.; Chen, J. T.; Mao, G.; Ober, C. K.; Thomas, E. L. *Polymer* **2000**, *41*, 8897.

(6) (a) Zheng, W. Y.; Hammond, P. T. *Macromolecules* **1998**, *31*, 711. (b) Zheng, W. Y.; Albalak, R. J.; Hammond, P. T. *Macromolecules* **1998**, *31*, 2686. (c) Anthamatten, M.; Zheng, W. Y.; Hammond, P. T. *Macromolecules* **1999**, *32*, 4838. (d)

Wu, J. S.; Fasolka, M. J.; Hammond, P. T. *Macromolecules* **2000**, *33*, 1108.
(7) Li, M. H.; Keller, P.; Albouy, P. A. *Macromolecules* **2003**, *36*, 2284.
(8) (a) Zhou, Q. F.; Zhu, X. L.; Wen, Z. Q. *Macromolecules* **1989**, *22*, 491. (b) Zhang, D.; Liu, Y.; Wan, X.; Zhou, Q. F. *Macromolecules* **1999**, *32*, 5183. (c) Wan, X.; Tu, Y.; Zhang, D.; Zhou, Q. F. *Chin. J. Polym. Sci.* **1998**, *16*, 377. (d) Pragliola, S.; Ober, C. K.; Mather, P. T.; Jeon, H. G. *Macromol. Chem. Phys.* **1999**, *200*, 2338. (e) Gopalan, P.; Ober, C. K. *Macromolecules* **2001**, *34*, 5120.
(9) (a) Chen, J. T.; Thomas, E. L.; Ober, C. K.; Mao, G. P. *Science* **1996**, *273*, 343. (b) Kato, T. *Science* **2002**, *295*, 2414. (b) Klok, H. A.; Lecommandoux, S. *Adv. Mater.* **2001**, *13*, 1217. (c) Lee, M.; Cho, B. K.; Zin, W. *Chem. Rev.* **2001**, *101*, 3869.
(10) (a) Nakajima, A.; Hayashi, T.; Kugo, K.; Shinoda, K. *Macromolecules* **1979**, *12*, 840. (b) Lecommandoux, S.; Achard, M. F.; Langenwalter, J. F.; Klok, H. A. *Macromolecules* **2001**, *34*, 9100.
(11) (a) Zhong, X. F.; FranÁois, B. *Makromol. Chem., Rapid Commun.* **1988**, *9*, 411. (b) Widawski, G.; Rawiso, M.; FranÁois, B. *Nature (London)* **1994**, *369*, 387.
(12) Jenekhe, S. A.; Chen, X. L. *Science* **1999**, *283*, 372.
(13) Chen, J. T.; Thomas, E. L.; Ober, C. K.; Hwang, S. S. *Macromolecules* **1995**, *28*, 1688.
(14) (a) Stupp, S. I.; Lebonheur, V.; Walker, K.; Li, L. S.; Huggins, K. E.; Keser, M.; Amstutz, A. *Science* **1997**, *276*, 384. (b) Zubarev, E. R.; Pralle, M. U.; Li, L.; Stupp, S. I. *Science* **1999**, *283*, 523.
(15) (a) Wan, X.; Tu, Y.; Zhang, D.; Zhou, Q. F. *Polym. Int.* **2000**, *49*, 243. (b) Tu, Y.; Wan, X.; Zhang, D.; Zhou, Q. F.; Wu, C. *J. Am. Chem. Soc.* **2000**, *122*, 10201. (c) Tu, Y.; Wan, X.; Zhang, H.; Fan, X.; Chen, X.; Zhou, Q.-F.; Chau, K. *Macromolecules* **2003**, *36*, 6565.
(16) Gopalan, P.; Zhang, Y.; Li, X.; Wiesner, U.; Ober, C. K. *Macromolecules* **2003**, *36*, 3357.
(17) Wunderlich, B. *Thermal Analysis*; Academic Press: Boston, 1990.
(18) Hamley, I. W. *The Physics of Block Copolymers*; Oxford University Press: Oxford, 1998.
(19) Miller, R. L. In *Proceeding of the 17th International Symposium on Order in the Amorphous State of Polymers*; Keinath, S. E., Miller, R. L., Rieke, J. K., Boyer, R. F., Eds.; Plenum: New York, 1987; p 33.
(20) Kumar, S. *Liquid Crystals*; Cambridge University Press: Cambridge, 2001.
(21) De Gennes, P. G.; Prost, J. *The Physics of Liquid Crystals*, 2nd ed.; Clarendon: Oxford, 1993.
(22) (a) Tu, H. L.; Wan, X. H.; Liu, Y. X.; Chen, X. F.; Zhang, D.; Zhou, Q. F.; Shen, Z.; Ge, J. J.; Jin, S.; Cheng, S. Z. D. *Macromolecules* **2000**, *33*, 6315. (b) Yin, X. Y.; Ye, C.; Ma, X.; Chen, E. Q.; Qi, X. Y.; Duan, X. F.; Wan X. H.; Cheng, S. Z. D.; Zhou, Q. F. *J. Am. Chem. Soc.* **2003**, *125*, 6854.
(23) Alexander, L. E. *X-ray Diffraction Methods in Polymer Science*; Wiley: New York, 1969.
(24) (a) Leland, M.; Wu, Z.; Chhajer, M.; Ho, R. M.; Cheng, S. Z. D.; Keller, A.; Kricheldorf, H. R. *Macromolecules* **1997**, *30*, 5249. (b) Leland, M.; Wu, Z.; Ho, R. M.; Cheng, S. Z. D.; Kricheldorf, H. R. *Macromolecules* **1998**, *31*, 22. (c) Li, C. Y.; Ge, J. J.; Bai, F.; Zhang, J. Z.; Calhoun, B. H.; Chien, L. C.; Harris, F. W.; Cheng, S. Z. D. *Polymer* **2000**, *41*, 8953. (d) Romo-Uribe, A.; Windle, A. H. *Macromolecules* **1993**, *26*, 7100. (e) Romo-Uribe, A.; Windle, A. H. *Macromolecules* **1996**, *29*, 6246.

MA0354905